

OR2-1

電線被覆上における燃え拡がり限界のモデル化：周囲流速と燃え拡がり速度に依存する気相と固相の消炎支配因子について

Modeling of the flame spread limits over wire insulation materials : On the control factors of flame extinction in the gas phase and solid phase that depend on the ambient flow velocity and spread rate

金野 佑亮, 橋本 望, 藤田 修

Yusuke KONNO, Nozomu HASHIMOTO, Osamu FUJITA

北海道大学大学院工学院, Hokkaido University, Faculty of Engineering

1. Introduction

Currently, the Japan Aerospace Exploration Agency (JAXA) is promoting the Flammability Limits at Reduced-g Experiment (FLARE) project [1][2]. A key target of the FLARE project is to establish a methodology for estimating the flammability of solid materials in spacecraft environments based on ground testing. Limiting Oxygen Concentration (LOC) indicating a minimum oxygen concentration to maintain the self-sustained combustion over solid fuels is used as a representative index to assess the material flammability. The authors are developing a theory and an experimental method for the estimation of the LOC of the wire insulation material.

In the flame spread over electric wires, the forward heat conduction in a wire core and the curvature of the wire surface play important roles in the heat transfer mechanism during the flame spread process. Our previous work revealed that the forward heat conduction in the wire core is responsible for the extinction of the flame spreading over an electric wire because the heat loss caused by the forward heat conduction in the wire core and the flame spread rate cause a negative feedback loop in the system [3]. Further, several previous works reported that the heat loss from the gas phase is responsible for the radiation extinction of the flame spreading over a thin cylinder due to the reduction of the radiation heat loss from the solid surface [4][5][6].

In this paper, we discuss the flame spread model for the estimation of the limit condition of flame spread over electric wires. To take account of the forward heat conduction through the wire core, a flame spread model is developed based on one-dimensional energy balance equations for the solid phase during the steady flame spread process. Additionally, a unique dimensionless number is developed to evaluate the controlling factors of the flame extinction in the gas phase, i.e., the effects of finite-rate chemistry and radiation heat loss on the flame temperature.

2. Flame spread model

2.1 Energy balance equation

Figure 1 shows a conceptual description of the opposed flame spread over an electric wire. In the present study, the length of the pyrolysis zone (L_{py}) and the flame spread rate (V_f) are considered as unknown quantities to be solved. Further, we assumed that the wire insulation is completely burnt out in the flame and no insulation is left over after the flame

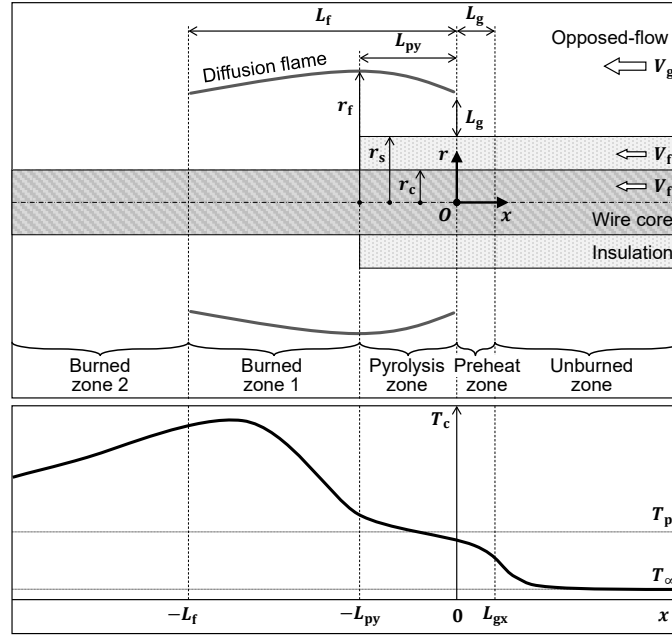


Fig. 1 Schematic description of opposed-flow flame spread over an electric wire and the temperature profile along a wire core during steady flame spread.

spread. Based on these assumptions, two equations that determine a set of solutions of L_{py} and V_f are derived by integrating the energy balance equation for the steady flame spread process as follows

$$g(L_{py}^*, V_f^*) = 0, \quad g(L_{py}, V_f) = \dot{Q}_{gs,py} + \dot{Q}_{cs,py} - \dot{Q}_{loss,py} - \rho_s A_s V_f \Delta h_v, \quad (1)$$

$$U(L_{py}^*, V_f^*) = 0, \quad U(L_{py}, V_f) = \dot{Q}_{input} - \dot{Q}_{loss} - \rho_s A_s V_f [\Delta h_v + c_{p,s}(T_p - T_\infty)]. \quad (2)$$

In Eqs. (1) and (2), $\dot{Q}_{gs,py}$ is the heat conduction from the gas phase to the insulation surface, $\dot{Q}_{cs,py}$ is the heat conduction from the wire core to the insulation, $\dot{Q}_{loss,py}$ is the heat loss from the insulation surface to the gas phase, ρ_s is the density of the insulation, A_s is the cross-sectional area of the insulation, Δh_v is the heat of vaporization of the insulation, \dot{Q}_{input} is the total heat input from the gas phase to the wire surface, \dot{Q}_{loss} is the total heat loss from the wire surface to the gas phase, $c_{p,s}$ is the specific heat of the insulation, T_p is the pyrolysis temperature of the insulation, and T_∞ is ambient temperature, respectively. Superscript * denotes the solution of the equation.

2.2 Extinction factor in the gas phase

It is well known that the residence time of the reactants and oxidizers in the reaction zone affects the temperature of the diffusion flame because of the finite-rate chemistry and the radiation heat loss from the flame. In the present study, a dimensionless number is developed from a nondimensionalized energy balance equation in the gas phase which includes a reaction term and heat loss term. The dimensionless number developed in this study is as follow.

$$\Omega = 1 - \frac{1}{Da} - H \quad (0 \leq \Omega \leq 1). \quad (3)$$

Da and H are the Damköhler number and heat loss parameter, respectively. Their relations to the dimensional counterparts are as follows

$$Da = \frac{\alpha_g \rho_g Y_{O_2, \infty} A e^{-E/(RT_f)}}{V_{g,eff}^2}, \quad (4)$$

$$H = \frac{h\lambda_g}{(\rho_g c_{p,g} V_{g,\text{eff}})^2}. \quad (5)$$

In Eqs. (4) and (5), α_g is the thermal diffusivity of the gas, ρ_g is the density of the gas, $Y_{O_2,\infty}$ is the mass fraction of oxygen in the oxidizer, A is the pre-exponential factor, E is the activation energy, R is the gas constant, T_f is the flame temperature, $V_{g,\text{eff}}$ effective opposed-flow velocity, h is the volumetric heat loss intensity that controls the magnitude of the radiation loss from the flame, λ_g is the thermal conductivity of the gas, and $c_{p,g}$ is the specific heat of the gas, respectively.

Ω in Eq. (3) becomes small in both high flow velocity and low flow velocity conditions. This behavior simulates the variation of the flame temperature with the residence time. Therefore, to evaluate the effect of residence time in the gas phase on the flame spread phenomenon, the heat input terms from the flame to the solid surface in the energy balance equations are multiplied by Ω . This method allows us to assess the effects of finite-rate chemistry and radiation heat loss on the flame spread phenomenon in a simple manner. To enable the quantitative estimation of the spread rate and LOC as a function of opposed-flow velocity using Ω , the values of A , E , and h in Eqs. (4) and (5) have to be tuned. In the present study, these parameters were optimized using the LOC obtained in both microgravity experiments and normal gravity experiments.

3. Results and discussion

3.1 Existence of multiple solutions for L_{py} and V_f and their stability

In this section, we discuss the characteristics of the solutions calculated by Eqs. (1) and (2) by looking at the representative calculation result at a particular condition. In the analysis, the thermochemical properties of low-density polyethylene (LDPE) insulated copper (Cu) wire were used since experimental data such as flame spread rates and LOC are available. The dimension of the wire is 0.5 mm wire core diameter and 0.15 mm insulation thickness. The ambient surrounding condition is set for 5 cm/s opposed-flow velocity and 17vol.% oxygen concentration.

Figure 2 (a) and (b) show mappings of $g(L_{py})$ and $U(V_f)$, respectively. As seen in the figures, because $g(L_{py})$ and $U(V_f)$ are nonlinear equations of L_{py} and V_f , they can have multiple solutions in a particular condition. By looking at the trend of $g(L_{py})$ and $U(V_f)$ in the vicinity of the solutions and considering constraints for L_{py} and V_f , we can understand the stability and the physical meaning of the solutions calculated by each equation.

In the present model, the wire insulation cannot be left over after the flame spread, thus, the solution of L_{py} must be smaller than the value of flame length. This is an important constrain for L_{py} . Additionally, the quantities of the $g(L_{py})$ and $U(V_f)$ imply the margin of the energy from the equilibrium state. Therefore, the dynamic responses of L_{py} and V_f

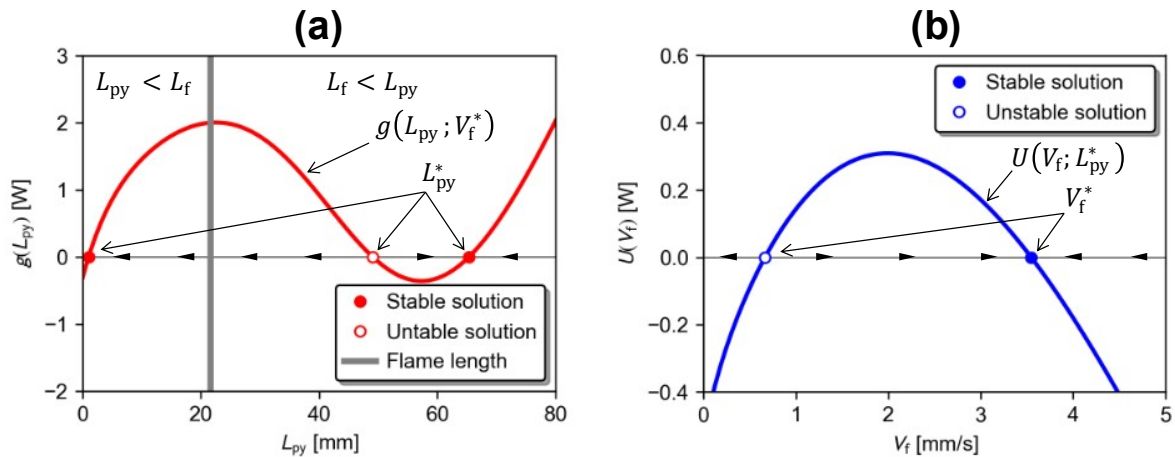


Fig. 2 (a) A mapping of $g(L_{py})$ and (b) that of $U(V_f)$. Electric wire considered in the analysis is LDPE insulated Cu wire with 0.5 mm core diameter and 0.15 mm insulation thickness. The ambient condition is set at 5 cm/s opposed-flow velocity and 17vol.% oxygen concentration.

can be understood based on the sign of $g(L_{py})$ and $U(V_f)$, respectively. Details of dynamic responses of L_{py} and V_f are summarized in Table 1. Additionally, because the dynamic responses of L_{py} and V_f in the vicinity of the solution were clarified, the stability of each solution can be determined based on the gradient of $g(L_{py})$ and $U(V_f)$ at the solution. The stabilities of the solutions depending on the sign of the gradient of $g(L_{py})$ and $U(V_f)$ are also summarized in Table 2. As presented in Fig. 2, $g(L_{py})$ in Eq. (1) can have three solutions but the smallest one is physically meaningful because others are large than the flame length. On the other hand, $U(V_f)$ in Eq. (2) can have two solutions, but the larger one is physically meaningful.

Table 1 The dynamic responses of L_{py} and V_f depending on the sign of $g(L_{py})$ and $U(V_f)$.

Sign of $g(L_{py})$	Response of L_{py}	Sign of $U(V_f)$	Response of V_f
$g(L_{py}) > 0$ (Excess energy)	Shrink	$U(V_f) > 0$ (Excess energy)	Accelerate
$g(L_{py}) = 0$ (Equilibrium)	Steady	$U(V_f) = 0$ (Equilibrium)	Steady
$g(L_{py}) < 0$ (Energy shortage)	Elongate	$U(V_f) < 0$ (Energy shortage)	Decelerate

Table 2 The stabilities of solutions of L_{py} and V_f depending on the sign of $g'(L_{py}^*)$ and $U'(V_f^*)$.

Sign of $g'(L_{py}^*)$	Stability of L_{py}^*	Sign of $U'(V_f^*)$	Stability of V_f^*
$g'(L_{py}^*) > 0$	Stable	$U'(V_f^*) > 0$	Unstable
$g'(L_{py}^*) = 0$	Quasi-stable	$U'(V_f^*) = 0$	Quasi-stable
$g'(L_{py}^*) < 0$	Unstable	$U'(V_f^*) < 0$	Stable

3.2 Effects of opposed-flow velocity and oxygen concentration on the flame spread rate

Since the characteristics of the solutions are revealed, we next investigate the effects of ambient conditions on the steady solution of the spread rate. Both stable and unstable solutions are plotted as a function of opposed-flow velocity for various oxygen concentrations in Fig. 3. For the Cu case, stable and unstable solutions are coincident in both high and low flow velocity conditions for various oxygen concentrations. The turning point shown in Fig. 3 is known as the fold bifurcation point and the characteristic of the bifurcation point well describes the actual flame behavior at extinction. Namely, we can understand that a turning point in high-flow velocity conditions and that in low-flow velocity conditions correspond to the blow-off extinction and radiation extinction, respectively. However, for the NiCr case, the radiation extinction was not observed in low flow velocity conditions for higher oxygen concentrations. Although it is not presented in this paper, this is because that the turning point of L_{py}^* appeared, then the model failed to determine the solution of the

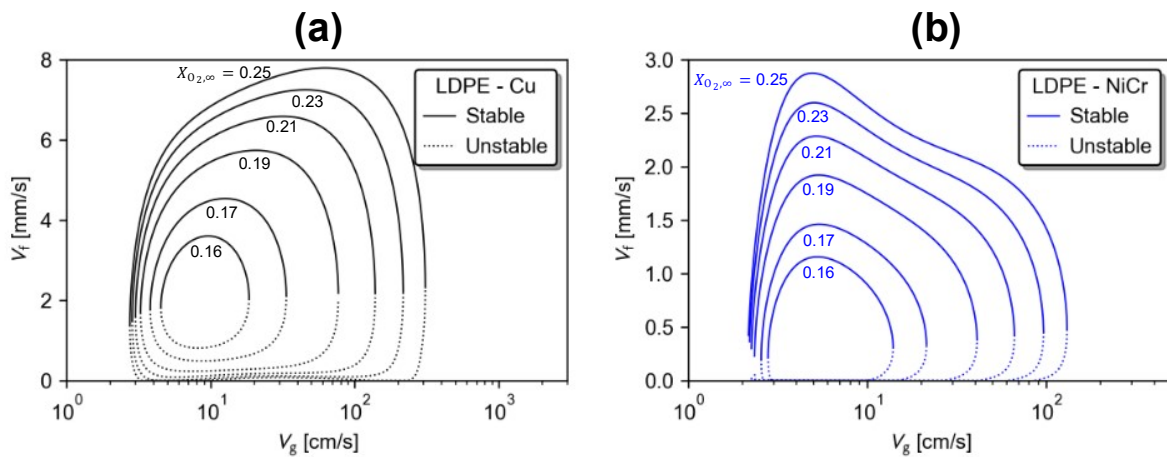


Fig. 3 Flame spread rate as a function of opposed flow velocity for various oxygen concentrations.

spread rate under this situation. The physical meaning of the turning point of L_{py}^* is the limit condition for the burnout of the wire insulation material during the flame spread process. Therefore, it does not correspond to the extinction of the spreading flame. This is one of the limitations of the present model. To predict the flame spread limit when the wire insulation is leftover during the spread process, the model has to be modified to allow the insulation leftover during the spread process and it will be future work in this study.

3.3 Flammability map

The variation of the blow-off extinction and radiation extinction with the oxygen concentration shown in Fig. 3 is plotted in Fig. 4 together with the experimental data. The experimental data were obtained under both microgravity [7][8] and normal gravity [9]. As seen in the figure, the right branch is the blow-off extinction branch while the left branch is the radiation extinction branch. The merging point of the two branches corresponds to the MLOC of the wire insulation material. As mentioned previously, although the model failed to predict the radiation extinction for NiCr wire under higher oxygen concentration, it does not affect the prediction of the MLOC. Although there are some discrepancies between the predictions and experimental data, the present model would be a useful model to understand the flammability limits of the wire insulation material in various opposed-flow velocity conditions.

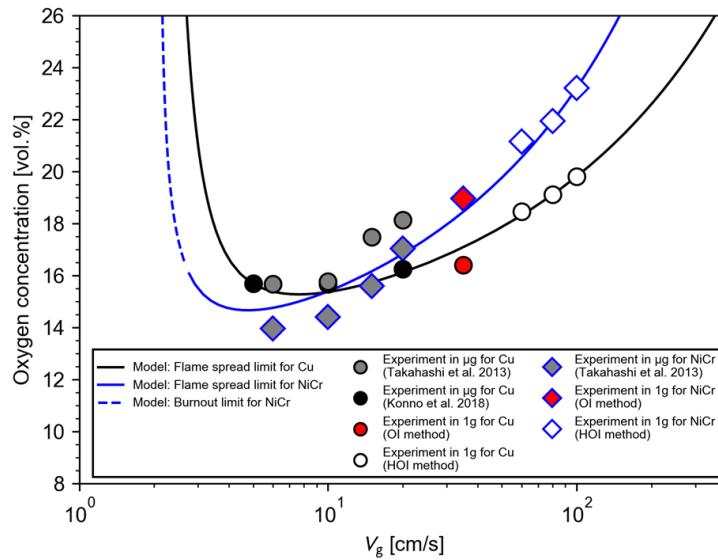


Fig. 4 Comparison of flame spread limits as a function of the opposed-flow velocity obtained by experiments and model.

4. Conclusions

A model of opposed flame spread over an electric wire is developed. The length of the pyrolysis zone (L_{py}) and the spread rate (V_f) are considered as the unknown quantities (eigenvalues) in the system and a set of two nonlinear equations are derived that determine the set of solutions of L_{py} and V_f . Both blow-off extinction and radiation extinction for the flame spreading over wire insulation material can be predicted based on the concept of the fold bifurcation point. The variation of the LOC obtained by the model and experiment showed good agreement in qualitative manner. We are currently studying the effect of the thermochemical properties of the wire insulation material on the LOC for the model validation. The result will be presented soon.

Acknowledgments

This research is supported by JAXA as a candidate experiment for the third stage use of JEM/ISS titled “Evaluation of gravity impact on combustion phenomenon of solid material toward higher fire safety” (called “FLARE”).

References

- [1] O. Fujita, Solid combustion research in microgravity as a basis of fire safety in space, *Proc. Combust. Inst.* 35 (3) (2015) 2487–2502.
- [2] M. Kikuchi, Overview of the “Solid Combustion” Experiment and the Solid Combustion Experiment Module, *Int. J. Microgravity Sci. Appl.* 32 (4) (2015) 320407.
- [3] Y. Konno, N. Hashimoto, O. Fujita, Role of wire core in extinction of opposed flame spread over thin electric wires, *Combust. Flame.* 220 (2020) 7–15.
- [4] M.A. Delichatsios, R.A. Altenkirch, M.F. Bundy, S. Bhattacharjee, L. Tang, K. Sacksteder, Creeping flame spread along fuel cylinders in forced and natural flows and microgravity, *Proc. Combust. Inst.* 28 (2) (2000) 2835–2842.
- [5] O. Fujita, K. Nishizawa, K. Ito, Effect of low external flow on flame spread over polyethylene-insulated wire in microgravity, *Proc. Combust. Inst.* 29 (2) (2002) 2545–2552.
- [6] L. Carmignani, A. Sato, S. Bhattacharjee, Flame spread over acrylic cylinders in microgravity: effect of surface radiation on flame spread and extinction, in: *48th Int. Conf. Environ. Syst.*, Albuquerque, New Mexico, 2018: pp. 1–7.
- [7] S. Takahashi, H. Ito, Y. Nakamura, O. Fujita, Extinction limits of spreading flames over wires in microgravity, *Combust. Flame.* 160 (9) (2013) 1900–1902.
- [8] Y. Konno, Study on Opposed-Flow Flame Spread and Extinction Phenomena of Solid Materials with Metal Conductor, Unpublished Master’s thesis, Hokkaido University, 2018.
- [9] M.Z.B.Z. Abidin, Development of blow off test for determination of limiting oxygen concentration of wire insulation materials: Observation of downward flame spread in the near-limit condition under high flow velocity condition, Unpublished Bachelor’s thesis, Hokkaido University, 2021.



© 2021 by the authors. Submitted for possible open access publication under the terms and conditions of the Creative Commons Attribution (CC BY) license (<http://creativecommons.org/licenses/by/4.0/>).